Recent Development in the Field of High Entropy Alloys

Kapil Dev, Vikas Kumar Singla, Shubham Tripathi, Md Salim Khan, Vivek Rathore, Sunny Kumar

Department of Mechanical Engineering, JSS Academy of Technical Education
Noida, Uttar Pradesh, India.

Abstract

In this article a review of current advancement in the field of High Entropy Alloys has been presented. Papers from various reputed journal has been summarized. High-entropy alloys (HEAs) are known for their unique mechanical properties, which include high tensile strength even at high temperatures, high hardness, toughness exceeding that of most pure metals and alloys, comparable strength to structural ceramics and some metallic glasses, exceptional ductility and fracture toughness at cryogenic temperatures, and corrosion resistance. A lot of research is going on HEAs due to their application in different fields.

Key Words: High Entropy Alloy (HEA), Mechanical Properties

Introduction

A metal alloy with proportions of five or more metallic components is known as a high-entropy alloy (HEA). Multi-principal metal alloys (MPEAs) are metal alloys that contain two or more fundamental elements. HEAs are a subset of MPEAs. HEAs, like MPEAs, are noted for having better physical and mechanical qualities than traditional alloys.

High-entropy alloys (HEAs) are known for their unique mechanical properties, which include high tensile strength even at high temperatures, high hardness, toughness exceeding that of most pure metals and alloys, comparable strength to structural ceramics and some metallic glasses, exceptional ductility and fracture toughness at cryogenic temperatures, and corrosion resistance. Complex concentrated solid solutions created by the suppression of fragile intermetallic complexes as a result of high mixing entropy and enthalpy values were attributed to all of these unique features [1]. When the mixing enthalpy and atomic size difference is modest, HEAs tend to form and make single-phase solid solutions.

As a result of these unique characteristics, HEA is now being considered as a material for a variety of applications, including structural applications, aerospace engineering, and civil transportation; superconducting electromagnets, such as magnetic resonance imaging, scanners, nuclear magnetic resonance machines, and particle accelerators; high-temperature applications, such as gas turbines, rocket nozzles, and nuclear construction; and cryogenic applications, such as roentgen synthesis..

Due to the diversification of types of interventions in military activities, the specifications on the security of collective protection equipment and structures in the military field have increased the requirements for the resistance of protection panels/floors/elements to penetration by various types of

projectiles. The highest possible breaking and yield strength values, the highest possible hardness and impact resistance, and the highest possible elongation at break and energy absorbed by a notched specimen while breaking under an impact load (the Charpy test) at temperatures as low as minus 40°C are the main characteristics of materials intended for the manufacture of protection components. Current military specifications call for hardness levels of at least 540–600 BHN (Brinell hardness) or 55–60 HRC (Rockwell hardness), as well as yield and breaking strength values of at least 1500 and 1700 MPa, respectively. When utilising the Charpy test to determine impact fracture energy, the values must be around 13 J at 40 °C, with elongations of at least Such requirements have been met by designing metallic alloys of various compositions; the most widely used is the high-strength microalloyed steels, used to produce reinforcement elements of thicknesses between 8.5 and 30 mm. Some research papers in the military field [4] have shown that the hardness of the plating material is not a sufficient factor to provide maximum resistance against penetration by projectiles, considering that the values of the mechanical strengths (yield and breaking) are much more important in the behaviour process under dynamic stress.

For military applications, high-entropy alloys from the AlCrFeCoNi system have excellent mechanical qualities. As a result, the yield stress, compressive strength, and plastic deformation of these alloys reach unexpectedly high levels, making them suitable for use as composite structures resistant to dynamic stresses with high deformation velocity, such as in collective protection [9-20].

**Mechanical properties of some high-entropy alloys**

Alloy	Yield Strength (MPa)	Compressive Strength (MPa)	Plastic Deformation (%)
AlCrFeCoNi	1250.96	2004.23	32.7
CrFeCoNiCuTi	1272	1272	1.6
AlCrMnFeCoNiCuTiV	1862	2431	0.95
CrFeCoNiCuTi$_{0.5}$	700	1650	21.26

Since the first copper-based alloy was cast over 7000 years ago, metallurgy has been based on the production of alloys in which one metal, the base alloy, was used as the host for additional metals (alloying elements) to ameliorate the base metal's potential weaknesses. Because most metals are ductile, the objective of alloying elements is to increase hardness and strength. As society became more sophisticated, it began to demand more metallic materials, and new requirements such as corrosion resistance, wear resistance, high temperature resistance, fatigue resistance, impact resistance, and so on were added.. These demands compelled physical metallurgists to create new material classes and heat treatments. In the 1970s, when a new class of materials called intermetallics was discovered industrially, the paradigm of a 'base metal' to construct an alloy began to shift. Intermetallics, with their defined stoichiometry and high hardness, play an essential role as secondary components after heat treatments. As a result of the search for materials with enhanced strength at high temperatures and low densities, several intermetallics, such as -TiAl, with a stable face-centred cubic (FCC) structure at room temperature, became available. However, these new families of alloys with no defined base element were limited to a few intermetallic families, where the major component was usually two separate metals combined. The use of alloying elements has always been limited, with the exception of the intermetallic

approach and 'superalloys,' where the number of alloying elements could reach half of the composition. This constraint is linked to the risk of uncontrolled intermediate chemicals developing, which can cause the material to become brittle.

This technique of working in physical metallurgy began to shift in 2004 when Cantor et al. presented a study in which they created a multicomponent alloy using five elements in equiatomic proportions (Fe20Cr20Mn20Ni20Co20) and achieved an FCC monophasic structure. Similarly, Yeh et al. developed the similar notion, describing 'high-entropy alloys' (HEAs) as alloys with five or more primary elements in equimolar ratios. To broaden the scope of the alloy design, Yeh et al. suggest that HEAs contain primary components in concentrations ranging from 35 to 5% for each element. In this study, Yeh et al. describe how managing the configurational entropy of the system allows us to achieve a single-phase solid solution with such a large number of alloying elements. In traditional metallurgy, the primary element is present, while the alloying elements are present in minor amounts. In HEA, five or more alloying elements with similar atomic percentages make up the alloy. This is what we wish to illustrate in the figure, where the size of the circles represents the contribution of the various alloying components in the final alloy. Alloying philosophy in conventional metallurgy and in HEAs.
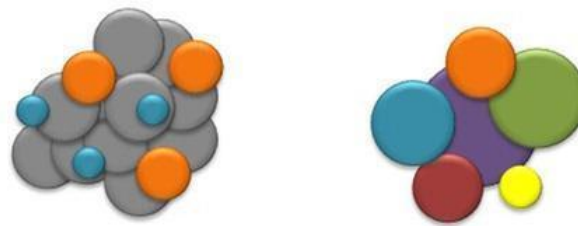
Conventional and High Entropy Alloy

According to the most comprehensive databases, HEAs have become a promising research subject, with over 5000 scholarly publications published. We'd like to highlight a few noteworthy evaluations from among those papers. The review of Miracle and Senkov [5], who developed a complete state of the art on the subject, is perhaps the most comprehensive. Their work covers concepts, fundamentals, alloy families, microstructural considerations, characteristics (including comparisons to competing alloys), and so on. This study is essential reading for scholars who are new to the field. There are a number of other general and critical reviews on the subject available in [6–10]. In addition, HEAs have been shown to be capable of displaying a wide range of features; numerous studies have compiled arguments highlighting their utility in various domains. The importance of HEAs in applications involving physical qualities such as magnetic, electrical, or thermal properties is highlighted in references [11, 12]. Under severely corrosive conditions, HEAs can also be utilised [13–15]. Furthermore, due to their superior mechanical performance [16–18], particularly at high [5] or cryogenic temperatures [19], HEAs are definitely a potential material for market introduction. Other studies of HEA mechanical behaviour focus on its basic deformation behaviour [20] or fracture resistance [21]. There have also been two books written on the subject [22, 23].

The majority of HEA-related research has focused on developing processing methods based on ingot metallurgy. When more than five metals, some of which have high melting points, must be melted and solidified with good solubility while avoiding segregation, arc melting has been proven to be a highly

effective procedure. However, ingot metallurgy offers significant challenges in cases where a complex composition is required, which may limit its potential for producing a developing, promising family of alloys. Powder metallurgy (PM) has showed great promise as a method of producing HEAs in this context. PM is a forming technology that can totally avoid segregation, provide superior microstructural control (including the generation of nanocrystalline materials), and readily make metal matrix composites.

Although the first articles on HEAs were published in 2004, it took another few years for papers employing PM to appear [24–26]. The merits of nanostructures and their prospective usage for numerous applications have been recognised since the early days of this novel family of structural alloys [4]. PM, like other forming techniques like high-pressure torsion, has significant advantages in this competitive context [27]. PM provides two additional advantages over conventional forming methods: (1) it can be utilised when metals of different densities are required, as when lightweight HEAs are formed [28]; and (2) it can be employed when a large number of metals with exceptionally high melting points are used in the production of the HEA, as in so-called refractory HEAs [29].

A selected search was conducted in four databases for this study (ISI Web of Science, Scopus, Science Direct and Google Scholar). Using various keyword combinations (high-entropy alloys, powder metallurgy, sintering, mechanical alloying (MA), gas atomising, and spark plasma sintering, among others), 166 papers that fulfilled the criteria were located. Some studies were excluded from the review database for the following reasons: a valid citation system could not be replicated, some steps in the experimental approach were unclear, or PM was employed as a substitute for other manufacturing processes. Many articles on 'laser cladding,' where powders were utilised to generate coatings or surface alterations on substrates using a laser power source, were found as an illustration of this latter difficulty. Papers were only used in these circumstances when the powder development played a unique function. Only a few studies were devoted to the development of powder technology, thus they were included for exceptional significance.

The growing number of papers published in the last ten years demonstrates the topic's importance (see the figure). The number of papers published over this time span has increased geometrically due to the growing interest in PM HEAs.
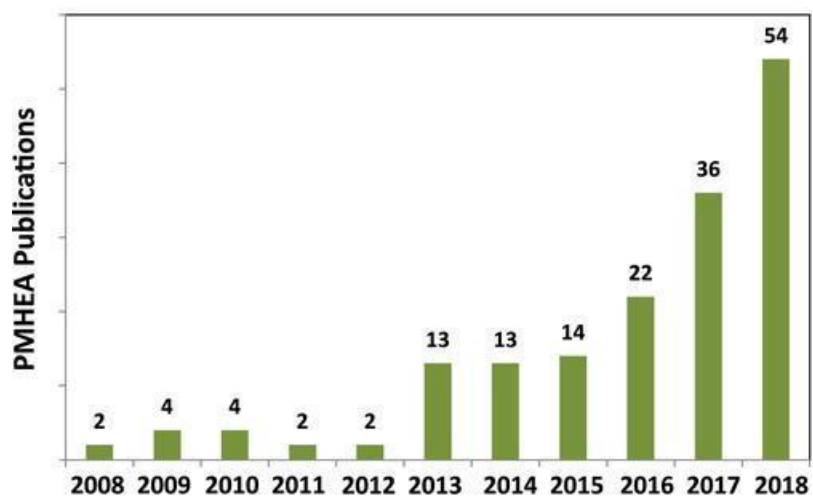
Research Papers Published In The Last 10 Years on PM HEAs

Ingot metallurgy was used to create the earliest HEAs, which consisted of at least five core elements alloyed in equimolar quantities. Hundreds of distinct compositions are available in the literature, most of which are based on 3d transition metals. To be called a HEA, such complex compositions (five or more elements, all of which play an essential role in the alloy) must meet a set of basic requirements specified by Yeh et al. [6]. These prerequisites are: (1) high-entropy effects in thermodynamics; (2) sluggish diffusion in kinetics; (3) severe lattice distortion in structures; and (4) properties: cocktail effects. These four core HEA effects have been thoroughly studied in various works, but [5, 18] and [30] highlight them.

According to the technical literature on ingot casting HEAs, they can be categorised into four groups: Transition metals in three dimensions, lightweight materials, lanthanide, and refractory HEAs are all examples.

HIGH ENTROPY ALLOYS

| 3d Transition metals	Lightweight materials	Lanthanide	Refractory
CoCrFeNi	AlTiVCr	HoDyYGdTb	NbCrMoTaTiZr
CoCrFeNiMn	MnAlZnCu(Mgx)	GdDyFrHoTb	AlNbMoTaV
CoCrCuFeNiTi	AlLiMgZnSn	GdErHoTb	AlMoNbTaTiZr
CoCrCuFeNiAl	AlLiMgScTi		WNbMoTaV

Classification of Ingot Metallurgy HEAs

Nearly 200 publications covering 166 PM alloys have been included in this evaluation. Because several writers employ the same alloys, the number of papers is higher than the number of alloys. When the frequency of different alloying elements is examined, three primary categories of elements emerge.

Distribution (frequency) of alloying elements in the studied PM HEAs (i.e. Fe is in 152 different alloys; Al in 98 of the studied alloys).
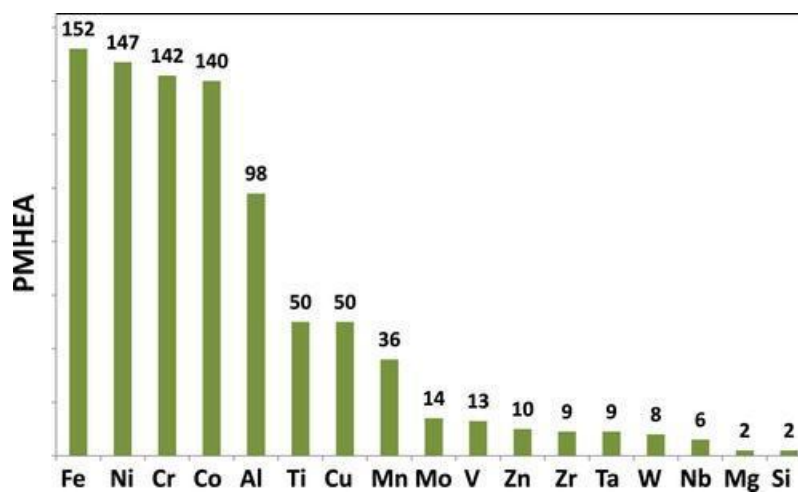
Main alloying elements in the HEAs studied
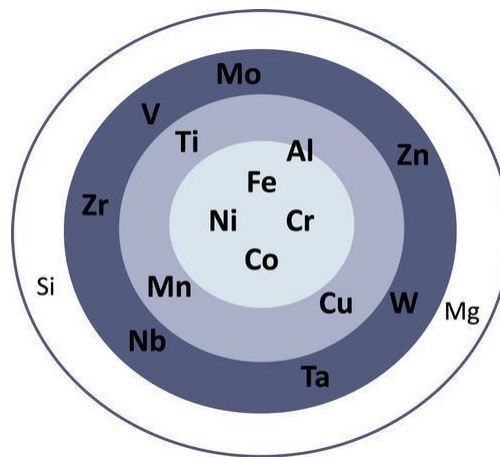
Main alloying elements in the HEAs studied

Fe, Ni, Cr, and Co are the most regularly used elements, all of which belong to the core group of transition metals. A second set of alloying elements, likewise pertaining to the transition metals (save Al), is employed less frequently: Al, Ti, Cu, and Mn. According to the definition of HEA proposed by Yeh et al. [4], at least five alloying elements are required. According to the figure, the majority of the alloys tested have four elements from the first group and one or two elements from the second group. Mo, V, Zn, Zr, Ta, W, and Nb are a third fascinating group of elements that are employed less frequently. Except for Zn, all of these components are refractory metals that play a key role in refractory HEAs [29]. Following the initial boom of HEAs based mostly on 3d transition metals, refractory HEAs were produced, with very particular and distinct features that could span a wider range of applications. Finally, certain examples of the utilisation of components such as Mg and Si are recounted, resulting in a fourth group in the figure.

We used the statistical Jaccard distance to run a hierarchical cluster analysis (HCA) to see if certain combinations of items were employed consistently. The grouping followed the complete linkage method based on dissimilarities between the different alloys' compositions. In the investigation, we used 166 PM HEAs from various articles.

The HCA identified nine different clusters of alloys based on their composition. Some of the clusters had a few members, and others were composed of a considerably higher number of members. As could be expected, the clusters with more members are related to the HEAs based on the 3d transition metals.
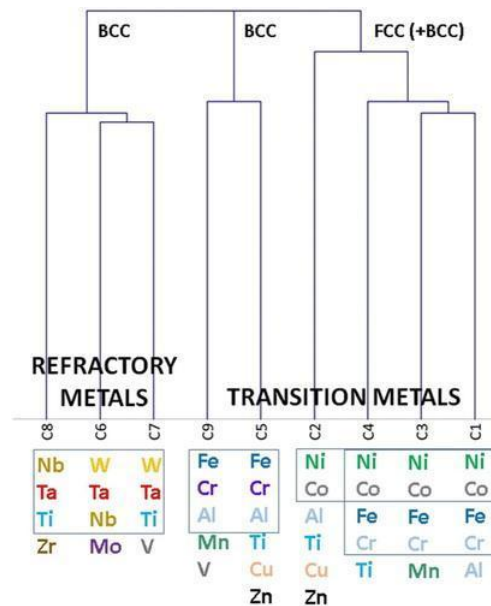
Dendrogram Showing The 9 types Of HEA Alloys Derived from the HCA

A bundle of papers can be seen on the right side of the tree diagram among clusters 1–3 and 4, and these latter groupings are tied to cluster 2. In terms of membership, these clusters are the most strong. The core group (clusters 1 and 3) is made up of four transition metals (Fe, Ni, Cr, and Co), which are the most prevalent in HEAs, plus a fifth transition metal from the second most commonly utilised elements (Al, Mn and Ti). Another intriguing fact is that cluster 3's core composition is the so-called Cantor alloy [3], which is one of the most studied HEAs in the field. If we look at the alloys in these clusters closely, we can see that most of them have an FCC structure after consolidation or, in certain cases, an FCC+body-centred cubic structure (BCC). Cluster 1's main composition exemplifies how Al is a crucial element that can significantly alter the crystal structure. The final crystal structure can be changed from FCC to FCC+BCC and BCC simply by altering the Al concentration in the HEA [6]. These four clusters are linked to Cluster 2, which shares only Ni and Co with the other clusters, as well as some other elements that vary by cluster, such as Al and Ti, but also Cu and Zn. Cluster 2 has elements in common with Ni, Co, Al, and Ti. These combinations of elements also produce a final structure of FCC+BCC in all the members of the cluster.

Three clusters on the left side of the dendrogram contain all of the refractory elements, including Ti. Because all of these elements have a BCC structure, all HEAs derived from various combinations of these elements should also have a BCC structure. These are also transition metals, with the majority belonging to Periods 5 and 6. These HEAs were created in the hunt for high-temperature load-bearing structures and thermal protection materials for the aerospace sector, among other applications [29, 178].

Two clusters in the dendrogram's centre are made up mostly of alloying elements from 3d transition metals. Fe, Cr, and Al are found in clusters 5 and 9, as well as Ti, Cu, Zn, Mn, and V. Many elements in these two clusters have a preference BCC structure, hence these HEAs will preferentially crystallise as BCC.

Powder Development

Obtaining suitable powders for the process is the first stage in every PM process. Using fully prealloyed powders as the starting material should make any PM approach easier in this specific family of alloys

where at least five separate metals contribute to the alloy. However, we identified several articles [33, 49, 52, 69, 80, 83] in which the starting point is a traditional powder mix with pure metals in powder form. The powders were subjected to various shape processes such as uniaxial pressing, cold isostatic pressing, and spark plasma sintering in those studies.

In the several studies that used fully prealloyed powders, two different techniques of obtaining the powders were used: MA and atomising. MA is the most frequent method for obtaining HEA powders. With enough time and energy to combine the best powder with the best composition, this process makes any imaginable composition viable. Appendix A displays the varied conditions utilised to create distinct totally prealloyed powders by MA, as well as the phase acquired when the process is done, in Table S1 of the accompanying supplemental data. The key records of this table are shown in the figures. The main milling system is a planetary ball mill, using stainless-steel vials and balls as the main grinding mechanism, however various combinations are acceptable.
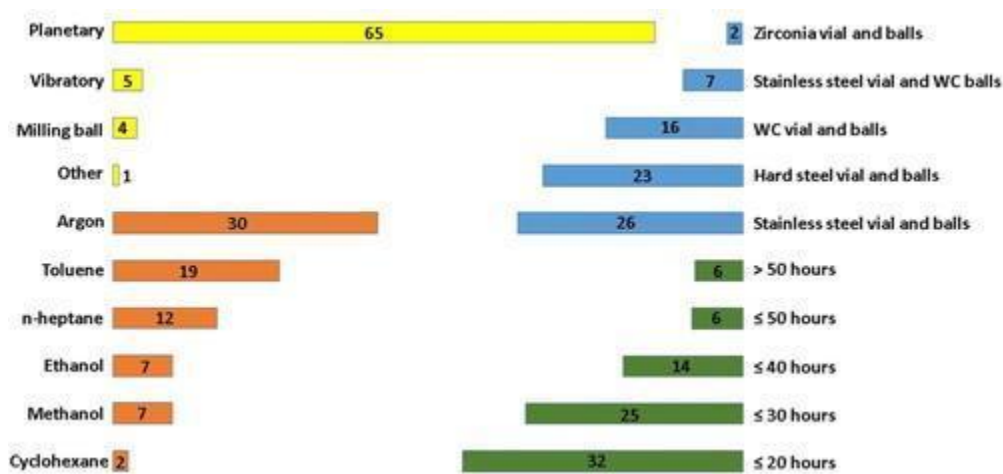
The length of the bars represents the number of times a certain procedure was used
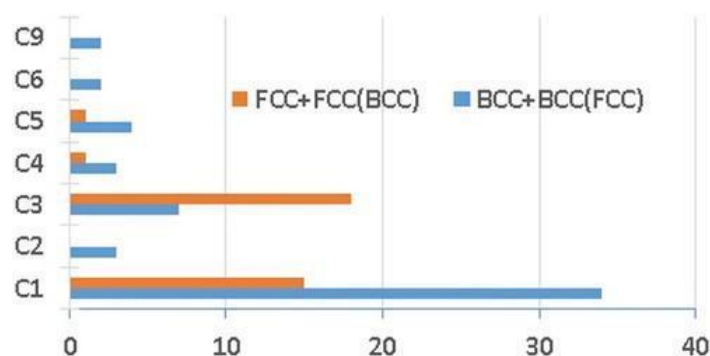
Frequency of the main phases associated to the clusters' compositions, obtained after the mechanical alloying step: BCC, FCC and BCC with some minor FCC and FCC with some minor BCC

A protected milling environment was applied in every case. Different writers have chosen different techniques to reach the best powder for the procedure depending on the alloy composition target. One important issue is that while most works use a carbon-based process control agent (PCA), only a few writers address contamination or impact in the final development of the HEA, as stated in the next paragraph..

After a prudential time for the procedure, i.e. on the order of hours, a monophasic HEA (BCC or FCC, depending on the starting metal powder) is formed in all of the examined articles. The leaving phases in clusters C1 to C4 are FCC and BCC, while in clusters C5 to C9, a BCC structure arises preferentially from the powder state and before any heat treatment..

One MA flaw to address is the possibility of powder contamination from two sources: the PCA and the grinding media. When the grinding media is stainless steel and the target alloy contains Cr and/or Fe, the transfer of these elements can be regulated, similar to how tungsten carbide is used to make some refractory HEAs. Nonetheless, the PCA's effect is not insignificant and is not acknowledged in the majority of the studies examined. Only two articles [144] consider the effect of the PCA, minimising it due to the potential creation of unwanted carbides during the formation process by spark plasma sintering (SPS).In contrast, in other works, the presence of extra carbon is desirable because the final goal of the process is to develop a hardmetal from the HEA [141].

Atomising is the second most frequent method for obtaining a fully prealloyed HEA powder. Most additive manufacturing processes are well-suited to this PM method. Various atomising procedures are discussed in this review, all of which have yielded positive results: gas atomising in Ar [73, 107, 108, 121, 140], gas atomising in N2 [59], and even water atomising.

[61, 70] used an alternative to MA and atomization to obtain fully prealloyed HEA powders. Melting alloys was used in those experiments, and the as-cast bulk portion was then pulverised using high-energy milling.

We must mention the work of Liu et al. [124] to complete this chapter on powder development. A hardmetal based on the HEA binder was pursued in their research. WC, Mo2C, TaC, NbC, and VC were blended with pure Ti in a high-energy mill instead of using pure elemental powders as the starting powders for the alloying elements of the binder and then combining these powders with the reinforcing carbide (this time TiC). SPS sintered the combined powders at a high temperature (1500 °C), taking into account the increased affinity of Ti for C and searching for the reduction of all refractory carbides at the sintering temperature. At the end of the process, a matrix of BCC HEA with TiC as the reinforcing agent was obtained.

Mechanical Behaviour of HEAs

If we classified high-entropy materials into a distinct family in the material world, it must be as a 'structural material,' and in this family of materials, mechanical behaviour is probably the most significant attribute required. Some of the figures included in this paper were derived from a variety of sources. Despite the fact that all of the cited papers used standard tests to measure mechanical properties, it was not possible to ensure that all of the results were obtained using the same procedures (especially in the case of hardness, where the load in the Vickers hardness was different in most of the examined works). In this way, readers are aware that this data must be handled with caution.

Fine Grain and Twinning Effect

The studies on HEAs published by PM show that the strengthening processes that work in the alloys are necessarily the same as those that act in conventional HEAs. The impact of solid solutions in alloys containing at least five separate alloying elements with various structural properties is critical. The high

amount of alloying elements causes significant lattice distortions, which can have a significant impact on phase transformation, dislocation dynamics, and HEA yield. A detailed book that provides a basic grasp of this essential problem was just released [116]. However, even if the solid solution effect is ignored, the observed twinning after deformation is critical in HEAs. Most HEAs have an FCC structure, at least partially, that causes a twinning effect following deformation, which gives an extra deformation mode that boosts ductility. Twinning also creates additional interfaces inside the grains during deformation, resulting in a 'dynamic Hall-Petch' effect that accelerates work hardening and, as a result, enhances strength [137]. The intricate interaction between dislocations and twin boundaries can also be linked to the strengthening mechanism of nanoscale twins. Twin boundaries, especially when the thickness of the twin/matrix lamellae is reduced to the nanoscale, are thought to effectively inhibit dislocation motion, amplifying the Hall–Petch effect [122]. When the high lattice deformation is combined with the twinning effect, and we consider that twinning occurs in materials with a low stacking fault energy (SFE), the increase in solute atoms reduces the SFE significantly and increases the nanotwinning tendency [99]. These effects have been investigated extensively in ingot metallurgy HEAs, but they have also been verified in PMHEAs.

[34, 99] describes the twinning effect in the alloys CoNiFeAl0.6Ti0.4, CrCoNiFeAl0.6Ti0.4, and Al0.5CrFeNiCo0.3C0.2 produced by MA and SPS, respectively. The transmission electron microscopy (TEM) photographs show the FCC phase with nanoscale twins, as well as the associated selected-area electron diffraction (SAED) patterns. Energy dispersive X-ray spectroscopy (EDS)/TEM and the accompanying diffraction patterns indicated that the nanoscale twins were only detected in the FCC phase.
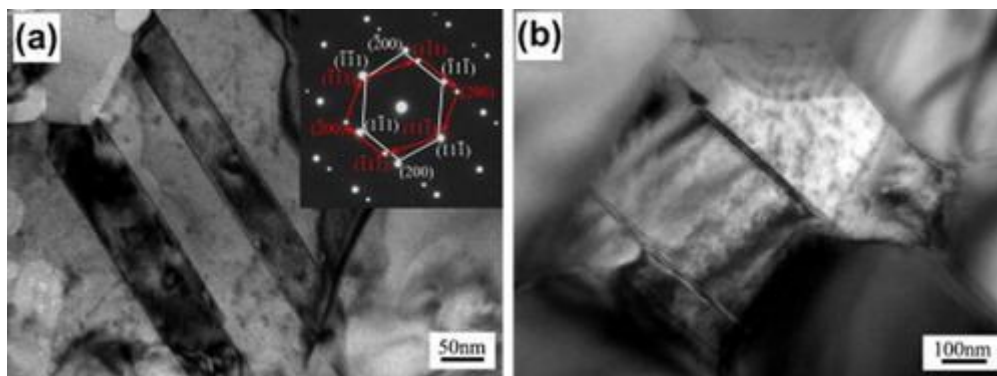
TEM microstructures and SAED pattern of a twinned FCC phase. (a) A twinned FCC grain with the corresponding SAED pattern, and (b) a twinned FCC grain surrounded by Cr23C6 carbide.

[55] also looked at the twinning effect in an AlCrCuFeNiZn HEA made by MA. The solubility of Cu and Zn FCC with other solute atoms causes stacking defects in this HEA. The twin thicknesses in a copper-aluminum alloy reduced as the Al percentage increased [130, 138]. Another significant element to consider is that the twinning effect under stress is mostly created in the compression mode, since tensile load twinning is minor [13].

Some PMHEA experiments suggest that there are more ways to boost the twinning effect. The introduction of reinforcing particles such as TiC [62] is one option. SFE is reduced when particles that can act as hard hinges in the production of deformation twins are introduced. The presence of dual microstructures is another option. Dual microstructures may be formed more easily with PM than with

other processing techniques, and dual microstructures may be useful for integrating BCC and FCC structures in PMHEAs [174]. A bimodal particle size distribution or ultrafine-grained microstructure could encourage the formation of dislocations, resulting in a high strain-hardening rate [22].

High-temperature Behaviour and High-strain-rate Deformation

Although HEAs are a promising material for use as structural materials at high temperature [23, 114], fewer articles deal with the behaviour of PMHEAs at high temperature.

A piece of Gleeble equipment dedicated to modelling thermomechanical treatments is used in several of these research to measure compression strength at various strain rates and temperatures. [104] investigates the behaviour of two alloys, TiNbTa0.5Zr and TiNbTa0.5ZrAl0.2, in compression at 800 °C with a 50% engineering strain. The influence on the microstructure of Nb and Ta precipitates, as well as the favourable effect of adding Al, are examined. The presence of precipitates in grain boundaries and the bimodal microstructure improve the mechanical behaviour at high temperatures in these alloys, which belong to the C8 cluster and have BCC as the main current phase. Another example is the CrFeCoNiMo0.2 (cluster C3) alloy study [109]. Specimens were tested at temperatures ranging from 700 to 1100°C in this case. Dynamic recovery and grain growth pinning by the precipitation of a Mo-rich phase improve the flow behaviour at high temperatures. In addition, there is some information on creep behaviour under compression. The compressive creep behaviour of an SPS-produced oxide-dispersion-strengthened (ODS) CoCrFeMnNi PMHEA was investigated in [123]. This research discovered that when the same material was tested with and without scattered oxides, the latter performed better. Few studies have looked upon tensile properties at high temperatures. In [119], MA and HP compare a unique PMHEA ($Fe18Ni23Co25Cr21Mo8WNb3C2$) with a 12 Cr ODS steel. The PMHEA steel has a substantially higher tensile strength but a poorer ductility than the ODS steel, as seen in the table.

Serrated yielding is a phenomenon that occurs when PMHEAs are subjected to a high strain deformation rate. This topic is visually explained in [98]. Varied compressive tests were done over a PMHEA in [133] (quasistatic at ambient temperature and different strain rates, quasistatic at different strain rates and different temperatures up to 900 °C, and dynamic compressive testing) (CoCrFeMnNi). This phenomena is more accurate in PMHEA than in an as-cast HEA, according to [21]. The periodic pinning and unpinning process of dislocations in the grains produced by the quantity of dispersed Cr-rich phase particles causes the serrations seen on the stress-strain curves of the PM CoCrFeMnNi HEA. Serration yielding is also increased by a rapid deformation rate at room temperature [107]. In [98], where tests are performed a low strain rate, the serration behaviour is also observed but in this case, it is attributed to the Al_2O_3 reinforcements in the $Al_{0.4}FeCrCo_{1.5}NiTi_{0.3}$ PMHEA.
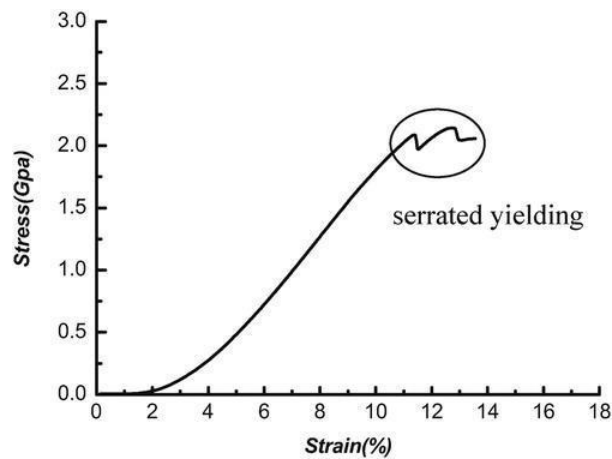
Stress-strain curve of $Al_{0.4}FeCrCo_{1.5}NiTi_{0.3}$ reinforced by nano-Al_2O_3 after SPS under compression

Compression Behaviour

The majority of articles on mechanical behaviour use compression tests to assess mechanical behaviour. As a result, extensive data can be used to analyse this subject. The results for yield strength, ultimate strength, deformation at fracture, and hardness for numerous HEAs, including HEA produced by ingot casting [53, 66], are included in Table S6 of the accompanying supplemental data, Appendix A. The alloy composition, the cluster to which the alloy belongs, the findings for these qualities, and the source of the data are all listed in the table. In addition, for comparison, the processing method used to obtain the alloy is mentioned (i.e. if it is a PM route another specific route, or casting).

The results of the ultimate compressive strength as a function of fracture deformation are shown. When these two qualities are analysed and compared in the figure, no discernible trend can be seen that could distinguish the materials obtained by conventional ingot casting from those obtained by PM. Perhaps the most notable distinction is that some HEAs made by casting have a relatively low deformation at fracture but a higher ability to achieve higher levels of deformation, but the sample of articles examined in this graph prevents us from drawing definite conclusions. collects just the results that belong to a given cluster, that is, according to the composition, without taking into account whether the processing is PM or ingot casting. Materials from clusters C1, C3, and C4, which are based on NiCoFeCr, are distributed across the image, demonstrating all possible strengths and deformations. On average, C3 materials have less strength (but can reach higher levels of deformation), while C4 materials have a lower level of distortion. They are based on the core group of transition metals (3d transition metals from the 4th period) commonly employed in ingot metallurgy and are the most common in the literature discussing HEAs. The Cantor alloy [3], which contains these elements plus Mn, was used to build HEAs in part. Leaving clusters C2–C5 (which have only one alloy) aside, materials constructed using clusters C6–C8, i.e. refractory HEAs, which are mostly constituted of refractory metals (W, Ta, Nb, Mo, Zr), show significantly less deformation at fracture.

Ultimate compressive strength vs. deformation at fracture of different HEA

Ultimate compressive strength vs. deformation at fracture of different HEA

However, when we compare hardness to fracture deformation, we can see a modest improvement in the hardness/deformation relationship of the cast alloys compared to the PM alloys. In any case, these results are based on a variety of materials (even compositions) made under a variety of processing

conditions, and this is merely a trend. Clearly, PM can compete in most fields to provide possibly required properties. Interestingly, the compositions and processing conditions of PMHEAs can be modified for a customised application, in contrast with ingot metallurgy.
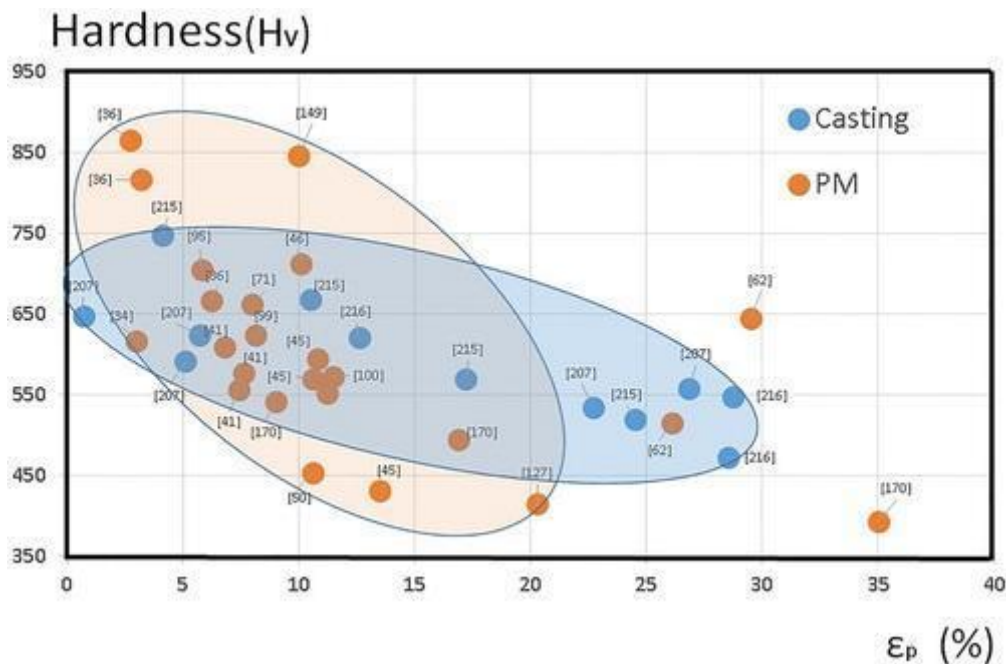
Hardness vs. deformation at fracture of different HEA

Tensile Behaviour

Unfortunately, there is very little knowledge about the tensile behaviour of PMHEAs. Only a few articles on tensile properties for these materials have been discovered. Some tensile results (those obtained from papers where reliable tensile data were provided) are shown in Table S7 of the accompanying supplementary data, Appendix A, as well as results from as-cast HEAs [34, 77, 111], rolled HEAs [26, 88, 102, 137], forged HEAs [109], and HEAs obtained by high pressure torsion [134]. Other structural alloys, such as Ti base alloys [35, 129], stainless steels [26], Ni base superalloys [54], ODS steels [87], or intermetallics [99], are also included in this category.

Some clusters of findings can be detected in the figure if we plot some of these results for analysis. Because these materials are the traditional structural alloys in this smaller range, as-cast HEAs can be found in all of the spaces of the figure, but might be appreciated in some groupings in the high values of deformation (and here Ti-based alloys show a little slightly bit better performance). The PMHEAs are dispersed over the space of the graph, just as they are in the compression findings, but this is irrelevant here because of the small amount of samples. Only one paper [77] examined the same material (CoCrFeNi HEA) manufactured by additive manufacturing and arc melting, and the results for the PMHEA are clearly positive (max/ in PMHEA of 745 MPa/32% vs. 457 Mpa/50% vs. 188 MPa, yield strength of 600 MPa vs. 188 MPa). Furthermore, the majority of the tensile results for the PMHEAs came from additive manufacturing materials. These are promising results, but there is a significant dearth of knowledge on this method, making it an interesting niche to investigate.

Tensile features for different HEAs and other structural alloys

Special Properties of PM HEAs

HEAs clearly have a lot of potential as structural materials, mainly because of their key mechanical properties, but they also have a lot of other useful features as structural materials. Some of these skills are outlined below.

Corrosion and Oxidation

The presence in the composition of an alloy of more than 20% (wt.) Cr in combination with Ti and Al powerfully suggests possible good corrosion or oxidation behaviour. Among the works covered in this review, some of them focus on corrosion or oxidation, and among those, most of them belong to compositional clusters C1 to C4, in which Cr, Ti or Al are present.

Considering the HEAs in [32, 52, 54, 104], all of them belong to compositional clusters C1 and C2 made by conventional PM. Electrochemical corrosion is tested through potentiodynamic polarisation curves, and better performance than that of stainless steel 304 was observed in all of these works. In [132], the electrochemical behaviour of a C4 cluster was evaluated by measuring the pitting potential, the results were positive. This later work was devoted to the development of composites (HEA reinforced with SiC), and introducing reinforcements deteriorated the pitting corrosion behaviour.

In [104] the pitting corrosion of three alloys (a CuZr alloy, labelled E2, a CuZrAlTiNi HEA, labelled E5, and stainless steel 304, obtained by MA and SPS) is evaluated by electrochemical polarisation measurements using a potentiostat in an artificial sea water solution at a scan rate of 0.003 V s^{-1}. The

artificial sea water mainly consisted of NaCl, MgSO$_4$, MgCl$_2$ and CaCl$_2$. The corrosion resistance of the as-sintered bulk samples in the sea water solution is demonstrated by the potentiodynamic polarisation curves displayed in the figure. The HEA sintered at 620°C exhibits the highest corrosion potential (E$_{corr}$) and the lowest corrosion current density (i$_{corr}$) with a wider passive region. The HEA sintered at 959 °C possesses the best passivity behaviour (the lowest i$_{pass}$) and a high pitting resistance (with the widest passive region). The corrosion rate (r$_{corr}$) can be calculated through Faraday's law, as shown in the equation below:

$$R_{corr} = 0.0327 \times (EW \times i_{corr} \div D) \qquad (1)$$

Where EW is the equivalent weight, and D is the density. shows all these corrosion parameters (and also the pit potential and shows the best behaviour of the HEA sintered at 620 against the stainless steel, tested under the same conditions.
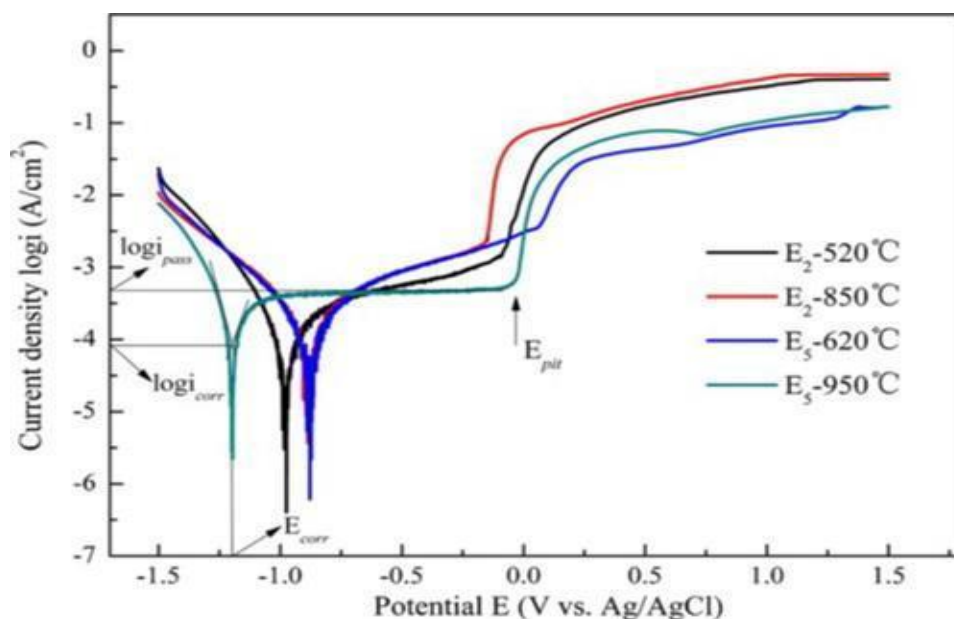
Potentiodynamic polarisation curves of the as-sintered E2 (CuZr alloy) and E5 (CuZrAlTiNi HEA) bulk alloys at different sintering temperatures (from 520 °C to 959 °C)

Only one work [84] has been found in which the behaviour of the HEA is less competitive than that of stainless steel 304, and the reason should be related to the different aging treatments that were applied to the material, this time manufactured by direct laser fabrication.

If the performance against corrosion is quite good, the response against oxidation at high temperature is truly promising. In [47], a cermet based on an HEA (C1 cluster) was studied, and the oxidation tests were performed at the same time as cermets manufactured using conventional Ni/Co binders. The behaviour in the HEA-based cermet is three times superior. Similar behaviour can be found in [54] wherein in addition to the electrochemical corrosion, oxidation was studied. A unique study on a refractory HEA (C7 cluster) made by additive manufacturing can be found in [11]. Here, the behaviour was studied at high temperature in air, and a good performance was observed, suggesting good possible fusion applications.

The results explained above suggest that the HEAs have good potential for a niche of applications requiring good corrosion/oxidation behaviour.

Friction

In the classification of attributes, friction and wear are commonly lumped together, but we'll separate them apart in the next paragraph. Significant improvements in the friction behaviour of the alloys have been made by making little changes to the composition of the HEA, which is possible because to the flexibility of the PM process. Friction behaviour is critical in a variety of applications, particularly bearings. The profile of materials discussed here is covered in the chapter [133] on composites based on HEAs (HEACMs). Because as-cast HEAs contain segregations, multiple phases, and brittle intermetallics at grain boundaries, all of which negatively affect ductility and toughness and damage the friction features of these alloys, the advantages of PM for the development of this family of materials are highlighted in this later work.

Yadav et al. [132, 142] carried out a fascinating experiment in which they added Bi and Pb dispersoids to two different HEAs, AlCrFeMnV (C9 cluster) and CuCrFeTiZn (C5 cluster), respectively. The friction coefficient was lowered in both situations, and the wear resistance was raised by about 20%. The mechanical properties of the basic HEA were not considerably changed in any situation. A similar work was carried out in [140] with the addition of Mo to a basic HEA (CoCrCuFe). The presence of Mo in the microstructure caused some precipitates to form, which changed the friction behaviour, reducing friction as the amount of Mo increased.

Zhang et al. [120, 128]'s research points in the same direction. The basis alloy in these investigations was the core alloy of the C1–C4 clusters (CoCrFeNi), with Ni coated with graphite, Ni coated with MoS2, and S added to the alloy (added as FeS). From ambient temperature to 800 °C, the friction and wear behaviour was investigated. Excellent self-lubrication behaviour and wear resistance were observed in all situations. At room temperature, the friction coefficient was always lowered, and wear performance increased up to five times. Furthermore, the mechanical qualities were not severely harmed. To end this section on the friction properties, an interesting work on the machinability of an HEA manufactured by AM [136] is discussed. Different machining conditions were applied to the CoCrFeNiMn alloy (C3 cluster), and the report concluded that with the suitable process combination, any practical surface quality and dimensional accuracy could be obtained.

Soft Magnetic Features

Ji et al. [105] investigated the PM HEA's soft magnetic properties (CoCrFeNiMn, C3 cluster). After 60 hours of MA, the particles' hysteresis curve shows soft magnetic characteristics. The saturation magnetization and remanence ratio values are higher and lower, respectively, than those reported in the literature for a similar cast alloy [56]. This finding suggests that the powder, as-milled, can be employed as a soft magnetic material. Furthermore, the powder displayed superparamagnetic behaviour, which has previously been observed for magnetic particles smaller than 10 nm [29]. Unfortunately, the coarsening of the grains following SPS changed the alloy's soft magnetic and superparamagnetic properties.
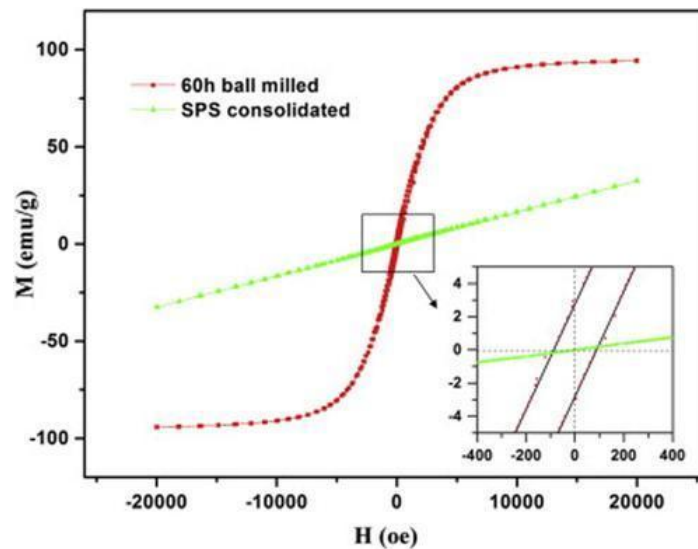
Magnetic hysteresis curves of the CoCrFeNiMn HEAs measured at room temperature.

Yu et al. [106] conducted a similar study, but this time with success in a PM consolidated HEA. In this research, changing just one element in the alloy changes the magnetic response dramatically. A similar result was obtained using the same alloy as Ji et al. [105], but the Mn in the composition was replaced with Cu (CoCrFeCuNi, also in the C3 cluster). Even after SPS, the saturation magnetization, remanence ratio, and coercivity levels allow this PM HEA to be used in soft magnetic applications. The saturation magnetization value achieved is higher than the CoCrFeNiCuTi HEA produced by casting [29].

These studies demonstrate that this is another promising field of application for PM HEAs.

Hydrogen Storage
Although hydrogen is regarded as a viable alternative to fossil fuels, its practical application is contingent on the development of materials capable of storing it. Some studies have shown that certain alloys with the BCC structure can react with hydrogen, making them a suitable hydrogen storage material [25]. With the right balance of alloying elements, several HEA compositions can guarantee the BCC structure. Kunce et al. [18] used additive manufacturing to create two PM HEAs with two distinct compositions (TiZrNbMoV and ZrTiVCrFeNi, which correspond to the C8 and C5 clusters, respectively), with the goal of utilising the BCC structure for hydrogen storage. Pressure-composition-temperature experiments were used to determine the viability of this possible application, and both alloys can absorb and desorb hydrogen (until the hydrogen is 1.8% and 0.59% in weight, respectively). The alloys were not able to completely desorbs hydrogen in this experimental configuration.

Pressure-composition-temperature experiments were used to determine the viability of this possible application, and both alloys can absorb and desorb hydrogen (until the hydrogen is 1.8% and 0.59% in weight, respectively). The alloys were not able to completely desorb hydrogen in this experimental configuration.

Conclusion
High-entropy alloys (HEAs) is having broad scope for research due to their unique mechanical properties, which include high tensile strength even at high temperatures, high hardness, toughness exceeding that of most pure metals and alloys, comparable strength to structural ceramics and some

metallic glasses, exceptional ductility and fracture toughness at cryogenic temperatures, and corrosion resistance. Worldwide a lot of research is going on HEAs due to their application in different fields.

Reference

1. Shechtman D, Blech I, Gratias D, & Cahn J W, Phys. Rev. Lett., 53. https://doi.org/10.1103/PhysRevLett.53.1951
2. Rawat R, Tiwari A, Arun N, Nageswara Rao S V S, Pathak A P, Shadangi Y, Mukhopadhyay N K, Rao S V, & Tripathi A, J Alloys Compd (2020) 157871. https://doi.org/10.1016/j.jallcom.2020.157871
3. Inoue A, Acta Mater 48 (2000) 279. https://doi.org/10.1016/S1359-6454(99)00300-6
4. Cantor B, Chang I T H, Knight P, & Vincent A J B, Mater Sci Eng A. 375–377 (2004) 213. https://doi.org/10.1016/j.msea.2003.10.257
5. Mukhopadhyay N K, Curr Sci 109 (2015) 665. http://www.jstor.org/stable/24905720
6. Murty B S, Yeh J W, & Ranganathan S, High-Entropy Alloys, 1st ed., Butterworth Heinemann, Oxford (2014)
7. Steurer W, Mater Charact 162 (2020) 110179. https://doi.org/10.1016/j.colsurfa.2020.124658
8. Shivam V, Basu J, Manna R, & Mukhopadhyay N K, Metall Mater Trans A Phys Metall Mater Sci 52 (2021) 15. https://doi.org/10.1007/s11661-021-06188-7
9. Jain H, Shadangi Y, Shivam V, Chakravarty D, Kumar D Shadangi Y, Shivam V, Chakravarty D, Mukhopadhyay N K, & Kumar D. J Alloys Compd 834 (2020) 155013. https://doi.org/10.1016/j.jallcom.2020.155013
10. Sriharitha R, Murty B S, & Kottada R S, Intermetallics 32(2013) 119. https://doi.org/10.1016/j.intermet.2012.08.015
11. Pandey V K, Shadangi Y, Shivam V, Basu J, Chattopadhyay K,Majumdar B, Sarma B N, & Mukhopadhyay N K, TransIndian Inst Met 74 (2021) 33. https://doi.org/10.1007/s12666-020-02114-4
12. Yadav T P, Mukhopadhyay S, Mishra S S, Mukhopadhyay N K, & Srivastava O N. Philos Mag Lett 0839 (2018) 1. https://doi.org/10.1080/09500839.2017.1418539
13. Chae M J, Sharma A, Oh M C, & Ahn B, Met Mater Int (2020)1. https://doi.org/10.1007/s12540-020-00823-5
14. KoKai T, YaChu Y, ChienChang J, TsungShune C, CheWei T, JienWei Y, Sci China Technol Sci 61 (2018) 184. https://doi.org/10.1007/s11431-017-9073-0
15. Yang X, Chen S Y, Cotton J D, Zhang Y, Jom 66 (2014) 2009.https://doi.org/10.1007/s11837-014-1059-z
16. Youssef K M, Zaddach A J, Niu C, Irving D L, Koch C C, MaterRes Lett 3 (2014) 95. https://doi.org/10.1080/21663831.2014.985855
17. Gao M C, Zhang B, Guo S M, Qiao J W, & Hawk J A, MetallMater Trans A Phys Metall Mater Sci 47 (2016) 3322. https://doi.org/10.1007/s11661-015-3091-1
18. Wang W H, Li H F, Qin L, Xie X H, Zhao K, Zheng Y F, & Wang Y B, Acta Biomater 9 (2013) 8561. https://doi.org/10.1016/j.actbio.2013.01.029
19. Li R, Gao J C, & Fan K, Mater Sci Forum 650 (2010) 265.https://doi.org/10.4028/www.scientific.net/msf.650.265
20. Li R, Gao J C, Fan K, Mater Sci Forum 686 (2011) 235. https://doi.org/10.4028/www.scientific.net/msf.686.235

21. Guo W, Neuefeind J C, Feng R, Zhang F, Hawk J A, Ren Y, Poplawsky J D, Liaw P K, Zhang C, & Gao M C, Acta Mater146 (2018) 280. https://doi.org/10.1016/j.actamat.2017.12.061

22. Chauhan P, Yebaji S, Nadakuduru V N, & ShanmugasundaramT, J Alloys Compd 820 (2020) 153367. https://doi.org/10.1016/j.jallcom.2019.153367

23. Mishra R K, & Shahi R R, J Magn Magn Mater 516 (2020).https://doi.org/10.1016/j.jmmm.2020.167342

24. Parameswaran P, Rameshbabu A M, Vijayan V, Sathish KumarG, Sakthivel C, Pargunam N, & Godwin Antony A, MetPowder Rep 75 (2020) 209. https://doi.org/10.1016/j.mprp.2019.08.001

25. Sharma A, Oh M C, & Ahn B, Mater Sci Eng A 797 (2020).https://doi.org/10.1016/j.msea.2020.140066

26. Cardoso K R, Roche V, Jorge Jr A, Antiqueira F, Zepon G, & Champion Y, J Alloys Compd 858 (2020) 158357. https://doi.org/10.1016/j.jallcom.2020.158357

27. Strozi R B, Leiva D R, Huot J, Botta W J, & Zepon G, Int JHydrogen Energy 46 (2021) 2351. https://doi.org/10.1016/j.ijhydene.2020.10.106

28. Maulik O, Patra N, Bhattacharyya D, Jha S N, & Kumar V,Solid State Commun 252 (2017) 73. https://doi.org/10.1016/j.ssc.2017.01.018

29. Khanchandani H, Sharma P, Kumar R, Maulik O, & Kumar V,Adv Powder Technol 27 (2016) 289. https://doi.org/10.1016/j.apt.2016.01.001

30. Maulik O, Kumar D, Kumar S, Fabijanic D M, & Kumar V,Intermetallics 77 (2016) 46. https://doi.org/10.1016/j.intermet.2016.07.001

31. Campos R P, Cuevas A C, & Mun˜oz R E, Mater Charact 110(2015) 1. https://doi.org/10.1007/978-3-319-15204-2

32. Fida Hassan S, Nadhreen G J, Al-Jeddawi M A A, Al-Otaibi M,Philos Mag Lett 100 (2020) 171. https://doi.org/10.1080/09500839.2020.1740810

33. Singh N, Shadangi Y, & Mukhopadhyay N K, Trans IndianInst Met 73 (2020) 2377. https://doi.org/10.1007/s12666-020-02039-y

34. Shivam V, Shadangi Y, Basu J, & Mukhopadhyay N K, JMater Res 34 (2019) 787. https://doi.org/10.1557/jmr.2019.5

35. Shivam V, Basu J, Pandey V K, Shadangi Y, & Mukhopadhyay N K, Adv Powder Technol 29 (2018). https://doi.org/10.1016/j.apt.2018.06.006

36. Shivam V, Basu J, Shadangi Y, Singh M K, & MukhopadhyayN K, J Alloys Compd 757 (2018). https://doi.org/10.1016/j.jallcom.2018.05.057

37. Shadangi Y, Sharma S, Shivam V, Basu J, Chattopadhyay K,Majumdar B, & Mukhopadhyay N K, J Alloys Compd (2020)154258. https://doi.org/10.1016/J.JALLCOM.2020.154258

38. Shadangi Y, Shivam V, Singh M K, Chattopadhyay K, Basu J, & Mukhopadhyay N K. J Alloys Compd 797 (2019) 1280.https://doi.org/10.1016/J.JALLCOM.2019.05.128

39. Shadangi Y, Shivam V, Varalakshmi S, Basu J, Majumdar B, Mukhopadhyay N K, Shivam V, Varalakshmi S, Basu J, Chattopadhyay K, & Mukhopadhyay N K, J Alloys Compd 834 (2020) 155065. https://doi.org/10.1016/j.jallcom.2020.155065

40. Mukhopadhyay N K, & Paufler P, Int Mater Rev 51 (2006)209. https://doi.org/10.1179/174328006X102475

41. Shadangi Y, Chattopadhyay K, Rai S B, & Singh V, SurfCoatings Technol 280 (2015) 216. https://doi.org/10.1016/j.surfcoat.2015.09.014

42. Shadangi Y, Chattopadhyay K, & Singh V, Jom 72 (2020)4330. https://doi.org/10.1007/s11837-020-04400-4

43. Basariya M R, Srivastava V C, & Mukhopadhyay N K, PhilosMag 6435 (2016) 1. https://doi.org/10.1080/14786435.2016.1204474

44. Raviathul Basariya M, Srivastava V C, & Mukhopadhyay N K,Mater Des 64 (2014) 542. https://doi.org/10.1016/j.matdes.2014.08.019

45. Zhang Y, Lu Z P, Ma S G, Liaw P K, Tang Z, Cheng Y Q, & Gao M C, MRS Commun 4 (2014) 57. https://doi.org/10.1557/mrc.2014.11

46. Guo S, Ng C, Lu J, & Liu C T, J Appl Phys 109 (2011) 1.https://doi.org/10.1063/1.3587228

47. Shivam V, Sanjana V, & Mukhopadhyay N K, Trans Indian Inst Met 73 (2020) 821. https://doi.org/10.1007/s12666-020-01892-1

48. Aravindh S A, Kistanov A A, Alatalo M, Komi J, Huttula M, & Cao W. J Phys Condens Matter (2020) 1. https://doi.org/10.1088/1361-648X/abda78

49. Gokhale A B, & Abbaschian G J, J Phase Equilibria 8 (1987)474. https://doi.org/10.1007/BF02893156

50. Maulik O, & Kumar V, Mater Charact 110 (2015) 116. https://doi.org/10.1016/j.matchar.2015.10.025

51. Cheng P, Zhao Y, Xu X, Wang S, Sun Y, & Hou H, Mater Sci Eng A 772 (2020). https://doi.org/10.1016/j.msea.2019.138681

52. V. Shivam, J. Basu, Y. Shadangi, M.K. Singh, & N.K.K. Mukhopadhyay: Mechano-chemical synthesis, thermal stability and phase evolution in AlCoCrFeNiMn high entropy alloy. J. Alloys Compd. 757, 87 (2018).

53. S. Varalakshmi, G. Appa Rao, M. Kamaraj, & B.S. Murty:Hot consolidation and mechanical properties of nanocrystalline equiatomic AlFeTiCrZnCu high entropy alloy after mechanical alloying. J. Mater. Sci. 45, 5158 (2010).

54. M. Omori: Sintering, consolidation, reaction and crystal growth by the spark plasma system (SPS). Mater. Sci. Eng., A 287, 183 (2000).

55. M. Murali, S.P. Kumaresh Babu, J. Majhi, A. Vallimanalan, & R. Mahendran: Processing and characterisation of nano crystalline AlCoCrCuFeTix high-entropy alloy. Powder Metall.61, 139 (2018).

56. S. Praveen, B.S. Murty, & R.S. Kottada: Alloying behavior in multi-component AlCoCrCuFe and NiCoCrCuFe high entropy alloys. Mater. Sci. Eng., A 534, 83 (2012).

57. S-H. Joo, H. Kato, M.J. Jang, J. Moon, E.B. Kim, S-J. Hong, & H.S. Kim: Structure and properties of ultrafine-grained CoCrFeMnNi high-entropy alloys produced by mechanical alloying and spark plasma sintering. J. Alloys Compd. 698, 591(2017).

58. P. Wang, H. Cai, & X. Cheng: Effect of Ni/Cr ratio on phase, microstructure and mechanical properties of NixCoCuFeCr2x (x 5 1.0, 1.2, 1.5, 1.8 mol) high entropy alloys. J. Alloys Compd.662, 20 (2016).

59. M. Vaidya, K.G. Pradeep, B.S. Murty, G. Wilde, & S.V. Divinski: Radioactive isotopes reveal a non sluggish kinetics of grain boundary diffusion in high entropy alloys. Sci. Rep. 7, 1 (2017).

60. S. Praveen, B.S. Murty, & R.S. Kottada: Phase evolution and densification behavior of nano crystalline multicomponent highentropy alloys during spark plasma sintering. JOM 65, 1797 (2013).

61. S. Praveen, A. Anupam, T. Sirasani, B.S. Murty, & R.S. Kottada: Characterization of oxide dispersed AlCoCrFe high entropy alloy synthesized by mechanical alloying and spark plasma sintering. Trans. Indian Inst. Met. 66, 369 (2013).

62. R.B. Mane, Y. Rajkumar, & B.B. Panigrahi: Sintering mechanism of CoCrFeMnNi high-entropy alloy powders. Powder Metall. 61, 131 (2018).

63. R.B. Mane and B.B. Panigrahi: Sintering mechanisms of mechanically alloyed CoCrFeNi high-entropy alloy powders. J.Mater. Res. 33, 3321 (2018).

64. R.B. Mane and B.B. Panigrahi: Comparative study on sinteringkinetics of as-milled and annealed CoCrFeNi high entropy alloy powders. Mater. Chem. Phys. 210, 49 (2018).

65. R.B. Mane and B.B. Panigrahi: Effect of alloying order on nonisothermal sintering kinetics of mechanically alloyed high entropy alloy powders. Mater. Lett. 217, 131 (2018).

66. E. Colombini, M. Lassinantti Gualtieri, R. Rosa, F. Tarterini,M. Zadra, A. Casagrande, & P. Veronesi: SPS-assisted synthesis of SICp reinforced high entropy alloys: Reactivity of SIC and effects of pre-mechanical alloying and post-annealing treatment. Powder Metall. 61, 64 (2018).

67. Z. Liu, Y. Lei, C. Gray, & G. Wang: Examination of solidsolution phase formation rules for high entropy alloys from atomistic Monte Carlo simulations. JOM 67, 2364 (2015).

68. Y. Zhang and Y.J. Zhou: Solid solution formation criteria forhigh entropy alloys. Mater. Sci. Forum 561–565, 1337 (2007).

69. S. Guo, C. Ng, J. Lu, & C.T. Liu: Effect of valence electronconcentration on stability of fcc or bcc phase in high entropy alloys. J. Appl. Phys. 109, 103505 (2011).

70. A. Kumar, P. Dhekne, A.K. Swarnakar, & M.K. Chopkar: Analysis of Si addition on phase formation in AlCoCrCuFeNi Six high entropy alloys. Mater. Lett. 188, 73 (2017).

71. S. Mohanty, T.N. Maity, S. Mukhopadhyay, S. Sarkar, N.P. Gurao, S. Bhowmick, & K. Biswas: Powder metallurgical processing of equiatomic AlCoCrFeNi high entropy alloy: Microstructure and mechanical properties. Mater. Sci. Eng., A 679, 299 (2017).

72. M. Zhang, W. Zhang, Y. Liu, B. Liu, & J. Wang: FeCoCrNiMo high-entropy alloys prepared by powder metallurgy processing for diamond tool applications. PowderMetall. 61, 123 (2018).

73. Y. Zhang, B. Zhang, K. Li, G.L. Zhao, & S.M. Guo: Electromagnetic interference shielding effectiveness of highentropy AlCoCrFeNi alloy powder laden composites. J. Alloys Compd. 734, 220 (2018).

74. J. Chen, P. Niu, T. Wei, L. Hao, Y. Liu, X. Wang, & Y. Peng: Fabrication and mechanical properties of AlCoNiCrFe highentropy alloy particle reinforced Cu matrix composites. J. Alloys Compd. 649, 630 (2015).

75. S. Praveen, A. Anupam, R. Tilak, & R.S. Kottada: Phaseevolution and thermal stability of AlCoCrFe high entropy alloy with carbon as unsolicited addition from milling media. Mater. Chem. Phys. 210, 57 (2018).

76. R.M. Pohan, B. Gwalani, J. Lee, T. Alam, J.Y. Hwang, H.J. Ryu,R. Banerjee, & S.H. Hong: Microstructures and mechanical properties of mechanically alloyed and spark plasma sintered Al0.3CoCrFeMnNi high entropy alloy. Mater. Chem. Phys. 210,62 (2018).

77. M. Vaidya, S. Armugam, S. Kashyap, & B.S.S. Murty:Amorphization in equiatomic high entropy alloys. J. Non-Cryst. Solids 413, 8 (2015).

78. Z. Fu, W. Chen, H. Wen, D. Zhang, Z. Chen, B. Zheng,Y. Zhou, & E.J. Lavernia: Microstructure and strengthening mechanisms in an FCC structured single-phase nanocrystalline Co25Ni25Fe25Al7.5Cu17.5 high-entropy alloy. Acta Mater. 107, 59 (2016).

79. L.H. Tian, W. Xiong, C. Liu, S. Lu, & M. Fu: Microstructure and wear behavior of atmospheric plasma-sprayed AlCoCrFeNiTi high-entropy alloy coating. J. Mater. Eng. Perform. 25, 5513 (2016).

80. W. Ji, J. Zhang, W. Wang, H. Wang, F. Zhang, Y. Wang, & Z. Fu: Fabrication and properties of TiB2-based cermets by spark plasma sintering with CoCrFeNiTiAl high-entropy alloy as sintering aid. J. Eur. Ceram. Soc. 35, 879 (2014).

81. H. Hadraba, Z. Chlup, A. Dlouhy, F. Dobes, P. Roupcova, M. Vilemova, & J. Matejicek: Oxide dispersion strengthened CoCrFeNiMn high-entropy alloy. Mater. Sci. Eng., A 689, 252 (2017).

82. Y. Liu, J. Wang, Q. Fang, B. Liu, Y. Wu, & S. Chen: Preparation of superfine-grained high entropy alloy by spark plasma sintering gas atomized powder. Intermetallics 68, 16 (2016).

83. M. Murali, S.P.K. Babu, B.J. Krishna, & A. Vallimanalan:Synthesis and characterization of AlCoCrCuFeZnx high-entropy alloy by mechanical alloying. Prog. Nat. Sci.: Mater. Int. 26, 380 (2016).

84. S. Mohanty, N.P. Gurao, & K. Biswas: Sinter ageing of equiatomic Al20Co20Cu20Zn20Ni20 high entropy alloy via mechanical alloying. Mater. Sci. Eng., A 617, 211 (2014).

85. A.I. Yurkova, V.V. Chernyavskii, & V.F. Gorban: Structure and Mechanical Properties of High-Entropy AlCuNiFeTi and AlCuNiFeCr Alloys Produced by Mechanical Activation Followed by Pressure Sintering. Powder Metall. Met. Ceram. 55, 152 (2016).

86. R.F. Zhao, B. Ren, G.P. Zhang, Z.X. Liu, & J. jian Zhang: Effect of Co content on the phase transition and magnetic properties of CoxCrCuFeMnNi high-entropy alloy powders. J. Magn. Magn. Mater. 468, 14 (2018).

87. Y. Tong, P. Qi, X. Liang, Y. Chen, Y. Hu, & Z. Hu: Differentshaped ultrafine MoNbTaW HEA powders prepared via mechanical alloying. Materials 10, 1 (2018).

88. A. Kumar, A.K.A.K. Swarnakar, & M. Chopkar: Phase evolution and mechanical properties of AlCoCrFeNiSix highentropy alloys synthesized by mechanical alloying and spark plasma sintering. J. Mater. Eng. Perform. 27, 3304 (2018).

89. H. Cheng, X. Liu, Q. Tang, W. Wang, X. Yan, & P. Dai: Microstructure and mechanical properties of FeCoCrNiMnAlx high-entropy alloys prepared by mechanical alloying and hotpressed sintering. J. Alloys Compd. 775, 742 (2019).

90. W. Guo, B. Liu, Y. Liu, T. Li, A. Fu, Q. Fang, & Y. Nie: Microstructures and mechanical properties of ductile NbTaTiV refractory high entropy alloy prepared by powder metallurgy. J.Alloys Compd. 776, 428 (2019).

91. D. Oleszak, A. Antolak-Dudka, & T. Kulik: High entropy multicomponent WMoNbZrV alloy processed by mechanical alloying. Mater. Lett. 232, 160 (2018).

92. V. Shivam, J. Basu, V.K. Pandey, Y. Shadangi, & N.K. Mukhopadhyay: Alloying behaviour, thermal stability and phase evolution in quinary AlCoCrFeNi high entropy alloy. Adv.Powder Technol. 29, 2221 (2018).

93. K.M. Youssef, A.J. Zaddach, C. Niu, D.L. Irving, & C.C. Koch: A novel low-density, high-hardness, high-entropy alloy with close-packed single-phase nanocrystalline structures. Mater.Res. Lett. 3, 95 (2014).

94. Q. Yang, Y. Tang, Y. Wen, Q. Zhang, D. Deng, & X. Nai: Microstructures and properties of CoCrCuFeNiMox high-entropy alloys fabricated by mechanical alloying and spark plasma sintering. Powder Metall. 61, 115 (2018).

95. L. Tian, M. Fu, & W. Xiong: Microstructural evolution of AlCoCrFeNiSi high-entropy alloy powder during mechanical alloying and its coating performance. Materials 11, 320 (2018).

96. Y. Long, K. Su, J. Zhang, X. Liang, H. Peng, & X. Li:Enhanced strength of a mechanical alloyed NbMoTaWVTi refractory high entropy alloy. Materials 11, 1 (2018).

97. D. Kumar, O. Maulik, S. Kumar, Y.V.S.S. Prasad, & V. Kumar: Phase and thermal study of equiatomic AlCuCrFeMnW high entropy alloy processed via spark plasma sintering. Mater. Chem. Phys. 210, 71 (2018).

98. K.B. Zhang, Z.Y. Fu, J.Y. Zhang, W.M. Wang, S.W. Lee, & K. Niihara: Characterization of nanocrystalline CoCrFeNiTiAl high-entropy solid solution processed by mechanical alloying. J.Alloys Compd. 495, 33 (2010).

99. S. Praveen, B.S. Murty, & R.S. Kottada: Effect of molybdenum and niobium on the phase formation and hardness of nanocrystalline CoCrFeNi high entropy alloys. J. Nanosci. Nanotechnol. 14, 8106 (2014).

100. F. Yuhu, Z. Yunpeng, G. Hongyan, S. Huimin, & H. Li: AlNiCrFexMo0.2CoCu high entropy alloys prepared by powder metallurgy. Rare Met. Mater. Eng. 42, 1127 (2013).

101. Z.Q. Fu, W.P. Chen, S.C. Fang, D.Y. Zhang, H.Q. Xiao, & D. Z. Zhu: Alloying behavior and deformation twinning in a CoNiFeCrAl0.6Ti0.4 high entropy alloy processed by spark plasma sintering. J. Alloys Compd. 553, 316 (2013).

102. Z. Fu, W. Chen, H. Xiao, L. Zhou, D. Zhu, & S. Yang: Fabrication and properties of nanocrystalline Co0.5FeNiCrTi0.5 high entropy alloy by MA-SPS technique. Mater. Des. 44, 535 (2013).

103. D. Kumar, O. Maulik, A.S. Bagri, Y.V.S.S. Prasad, & V. Kumar: Microstructure and characterization of mechanically alloyed equiatomic AlCuCrFeMnW high entropy alloy. Mater.Today: Proc. 3, 2926 (2016).

104. N.T.B.N. Koundinya, C. Sajith Babu, K. Sivaprasad, P. Susila,N. Kishore Babu, & J. Baburao: Phase evolution and thermal analysis of nanocrystalline AlCrCuFeNiZn high entropy alloy produced by mechanical alloying. J. Mater. Eng. Perform. 22, 3077 (2013).

105. S. Mridha, S. Samal, P.Y. Khan, K. Biswas, & Govind: Processing and consolidation of nanocrystalline Cu–Zn–Ti–Fe–Cr high-entropy alloys via mechanical alloying. Metall. Mater.Trans. A 44, 4532 (2013).

106. N.H. Tariq, M. Naeem, B.A. Hasan, J.I. Akhter, & M. Siddique: Effect of W and Zr on structural, thermal and magnetic properties of AlCoCrCuFeNi high entropy alloy. J. Alloys Compd. 556, 79 (2013).

107. F. Pru˚ša, A. Šenková, V. Kucera, J. Capek, & D. Vojt ech: Properties of a high-strength ultrafine-grained CoCrFeNiMn high-entropy alloy prepared by short-term mechanical alloying and spark plasma sintering. Mater. Sci. Eng., A 734, 341 (2018).

108. S. Fang, W. Chen, & Z. Fu: Microstructure and mechanical properties of twinned Al0.5CrFeNiCo0.3C0.2 high entropy alloy processed by mechanical alloying and spark plasma sintering. Mater. Des. 54, 973 (2014).

109. Yeh, J. W. & Lin, S. J. Breakthrough applications of high-entropy materials. J. Mater. Res. 33, 3129–3137 (2018).

110. Zhang, Y. High-Entropy Materials A Brief. Springer Singapore (2019).

111. Ching, W. Y. et al. Fundamental electronic structure and multiatomic bonding in 13 biocompatible high-entropy alloys. npj Comput. Mater. 6, 1–10 (2020).

112. Zhang, C. et al. Understanding phase stability of Al-Co-Cr-Fe-Ni high entropy alloys. Mater. Des. 109, 425–433 (2016).

113. Csaki, I. et al. Researches regarding the processing technique impact on the chemical composition, microstructure and hardness of AlCrFeNiCo high entropy alloy. Rev. Chim. 67, 1373–1377 (2016).

114. Yeh J W, Chen S K, Lin S J, Gan J Y, Chin T S, Shun T T, Tsau C H, & Chang S Y. Nanostructured high-entropy alloys with multiple principal elements: Novel alloy design concepts and outcomes. Adv. Eng. Mater. 6, 299-303+274 (2004). https://doi.org/10.1002/adem.200300567

115. Wang, Y. P., Li, B. S., Ren, M. X., Yang, C. & Fu, H. Z. Microstructure and compressive properties of AlCrFeCoNi high entropy alloy. Mater. Sci. Eng. A 491, 154–158 (2008).

116. Ye, Y. F., Wang, Q., Lu, J., Liu, C. T. & Yang, Y. High-entropy alloy: challenges and prospects. Mater. Today 19, 349–362 (2016).

117. Alabd Alhafez, I., Ruestes, C. J., Bringa, E. M. & Urbassek, H. M. Nanoindentation into a high-entropy alloy—an atomistic study. J. Alloys Compd. 803, 618–624 (2019).

118. Voiculescu, I., Geanta, V., Stefanoiu, R., Patrop, D. & Binchiciu, H. Influence of the chemical composition on the microstructure and microhardness of alcrfeconi high entropy alloy. Rev. Chim. 64, 1441–1444 (2013).

119. Li, Z., Zhao, S., Ritchie, R. O. & Meyers, M. A. Mechanical properties of high-entropy alloys with emphasis on face-centered cubic alloys. Prog. Mater. Sci. 102, 296–345 (2019).

120. Chen, C., Pang, S., Cheng, Y. & Zhang, T. Microstructure and mechanical properties of. J. Alloys Compd. 659, 279–287 (2016).

121. Yang, S., Liu, Z. & Pi, J. Microstructure and wear behavior of the AlCrFeCoNi high-entropy alloy fabricated by additive manufacturing. Mater. Lett. 261, 127004 (2020).

122. Chen, J. et al. A review on fundamental of high entropy alloys with promising high-temperature properties. J. Alloys Compd. 760, 15–30 (2018).

123. Miracle, D. B. & Senkov, O. N. A critical review of high entropy alloys and related concepts. Acta Mater. 122, 448–511 (2017).

124. Shon, Y., Joshi, S. S., Katakam, S., Shanker Rajamure, R. & Dahotre, N. B. Laser additive synthesis of high entropy alloy coating on aluminum: corrosion behavior. Mater. Lett. 142, 122–125 (2015)

125. Li, Q. H., Yue, T. M., Guo, Z. N. & Lin, X. Microstructure and corrosion properties of alcocrfeni high entropy alloy coatings deposited on AISI 1045 steel by the electrospark process. Metall. Mater. Trans. A Phys. Metall. Mater. Sci. 44, 1767–1778 (2013).

126. Zhou, P. F., Xiao, D. H. & Yuan, T. C. Microstructure, mechanical and corrosion properties of AlCoCrFeNi high-entropy alloy prepared by spark plasma sintering. Acta Metall. Sin. (English Lett.) 33, 937–946 (2020).

127. Yamanaka, K. et al. Corrosion mechanism of an equimolar AlCoCrFeNi high-entropy alloy additively manufactured by electron beam melting. npj Mater. Degrad. 4, 1–12 (2020).

128. Shi, Y. et al. Homogenization of AlxCoCrFeNi high-entropy alloys with improved corrosion resistance. Corros. Sci. 133, 120–131 (2018).

129. Shi, Y. et al. Corrosion of Al x CoCrFeNi high-entropy alloys : Al-content and potential scan-rate dependent pitting behavior. Eval. Program Plann. 119, 33–45 (2017).

130. Chen, H. Y. et al. Effect of the substitution of Co by Mn in Al-Cr-Cu-Fe-Co-Ni high-entropy alloys. Ann. Chim. Sci. Mater. 31, 685–698 (2006).

131. Feng, X. et al. Effect of Zr addition on microstructure and mechanical properties of CoCrFeNiZrx high-entropy alloy thin films.

132. Huang, Y. C., Su, C. H., Wu, S. K. & Lin, C. A study on the hall-petch relationship and grain growth kinetics in FCC-structured high/medium entropy alloys. Entropy 21, 297 (2019).

133. Geanta, V., Voiculescu, I., Vizureanu, P. & Victor Sandu, A. High entropy alloys for medical applications. Eng. Steels High Entropy Alloys (2020).

134. Qiu, Y. et al. Corrosion characteristics of high entropy alloys corrosion characteristics of high entropy alloys. Mater. Sci. Technol. 31, 1235–1243 (2015).

135. Guérin, M. et al. Identification of the metallurgical parameters explaining the corrosion susceptibility in a 2050 aluminium alloy. Corros. Sci. 102, 291–300 (2016).

136. Cao, L. et al. Microstructural evolution, phase formation and mechanical properties of multi-component AlCoCrFeNix alloys. Appl. Phys. A Mater. Sci. Process. 125, 1–11 (2019).

137. Krapivka, N. A., Firstov, S. A., Karpets, M. V., Myslivchenko, A. N. & Gorban, V. F. Features of phase and structure formation in high-entropy alloys of the AlCrFeCoNiCux system (x = 0, 0.5, 1.0, 2.0, 3.0). Phys. Met. Metallogr. 116, 467–474 (2015).

138. Baboian R. & Haynes, S. G. Cyclic polarization measurements-experimental procedure and evaluation of test data. (1981).

139. Chen, Y. Y., Duval, T., Hung, U. D., Yeh, J. W. & Shih, H. C. Microstructure and electrochemical properties of high entropy alloys—a comparison with type-304 stainless steel. Corros. Sci. 47, 2257–2279 (2005).

140. Liu, W. H., Wu, Y., He, J. Y., Nieh, T. G. & Lu, Z. P. Grain growth and the Hall–Petch relationship in a high-entropy FeCrNiCoMn alloy. Scripta Materialia 68.7, 526-529 (2013).